

Solubility and transport behavior of water and alcohols in NafionTM

D. Rivin^{*}, C.E. Kendrick, P.W. Gibson, N.S. Schneider

Natick Soldier Center, Natick, MA 01760-5020, USA

Received 21 February 2000; received in revised form 25 April 2000; accepted 25 April 2000

Abstract

Sorption isotherms, concentration dependent diffusion coefficients and immersion solubilities were determined for water and three alcohols (methanol, ethanol, propanol) at 32°C in acid-form NafionTM films. Apparent diffusion coefficients for water from vapor sorption kinetics exhibit a maximum at low concentrations, are higher for desorption than sorption and are below the reported immersion value. This anomalous behavior is attributed to nonisothermal conditions arising from the heat of condensation of water vapor and the time-dependent volume response to changes in vapor concentration, as well as, mass transfer limitations. To overcome these complications, diffusion coefficients were determined from steady state permeabilities combined with solubilities. Nominal diffusion coefficients, D_{nom} , from boundary layer corrected membrane resistances, exhibited characteristic differences in the magnitude and concentration dependence of the diffusion coefficient for water and the three alcohols, but D_{nom} for the liquids were far higher than for unit activity vapor. More detailed corrections for changes in the sweep and carrier vapor concentrations along the sample length and across the boundary layer were carried out to obtain effective diffusion coefficients, D_{eff} , with improved agreement between vapor and liquid. For water, D_{eff} increases smoothly and continuously with concentration. For the alcohols, D_{eff} exhibits three distinct regions of differing slope. These comparisons and the marked solubility increase with small amounts of water in the alcohols, suggest that water interacts more strongly with the sulfonic acid residues, while the alcohols preferentially solvate the fluoroether side chain and cause structural change which is responsible for the rapid D_{eff} increase in a narrow concentration range. © 2000 Elsevier Science Ltd. All rights reserved.

Keywords: Nafion; Ionomers; Transport behavior

1. Introduction

Polymer membranes which exhibit a high level of water vapor permeability, but are resistant to permeation by moderately polar organic molecules are of interest as light weight, permselective barrier materials. The well known perfluorosulfonate ionomer, NafionTM, was chosen for this study as a model system because of its extraordinarily high water permeability with only moderate water uptake, about 20% by weight by immersion at ambient temperature. Since the mechanism of water transport is related to the interactions with the ionic groups, it was expected that NafionTM might combine the properties of high water vapor permeability with the desired resistance to hazardous organic chemicals. NafionTM is currently employed in a wide variety of applications [1,2], including electrochemical processes, fuel cell membranes, coatings for ion selective electrodes, catalysis and pervaporative separations. The ionomer consists of a fluorocarbon backbone substituted with a low molar concentration of fluoroether side groups terminated

with the sulfonic acid residue. NafionTM is available as films of several different thicknesses, however, most published studies have employed NafionTM 117, a 178 μm film with an equivalent weight of 1100 g. This corresponds to substitution with one fluoroether-sulfonic acid side-chain for thirteen CF_2 groups whereby the side-chain amounts to 33% by weight of the polymer.

The main structural features of NafionTM arise from the incompatibility of the ion containing fluoroether side group and the nonpolar fluorocarbon backbone. The models of NafionTM structure differ in the nature and extent of phase segregation [3]. Based mainly on small angle X-ray scattering studies, the early model of Gierke [4,5], proposed that the sulfonic acid groups were clustered in spherical domains. The water swollen ionic domains were treated as inverse micelles, essentially pools of water, and it was proposed that water and ion transport occurred through narrow interconnecting channels. A more disordered model was developed by Yeager [6], which involved some intermixing of ionic groups in the interphase between the fluoroether ligand and the fluorocarbon matrix. This model also implies that the water and ion transports are restricted to the ion containing regions but does not impose

^{*} Corresponding author. Tel.: +1-508-233-4392; fax: +1-508-233-5223.
E-mail address: drivin@natick-amed02.army.mil (D. Rivin).

a regular geometric structure on these regions. Thus, passage through the predominant fluorocarbon regions would probably occur along random percolation pathways. The structure of NafionTM and the detailed mechanism of water transport and associated ionic conductivity are still active areas of research [3,7].

Although there have been several studies of the sorption and diffusion of water in NafionTM, the resulting data on the concentration dependence of the diffusion coefficient is less than satisfactory. The most extensive body of data is that of Morris and Sun [8] from sorption kinetics over a wide range of vapor concentrations and temperatures. The diffusion coefficient increases rapidly at low concentrations, but reaches a maximum at a concentration of about 0.07% (g/cm³), with a value of about 4×10^{-7} cm²/s at 25°C. The authors point out that their results, and other data cited from the literature, are lower than the value of 1.7×10^{-6} cm²/s at 25°C from measurements by liquid immersion determined in Eisenberg's laboratory [9]. Solvent self-diffusion coefficients of water in NafionTM, obtained by pulse field gradient NMR [10], also exhibited a maximum at a concentration of 0.07% when converted to "chemical" diffusion coefficients. These results are an order of magnitude higher than the Morris and Sun data at equivalent concentrations. At present there does not appear to be agreement on the magnitude or the concentration dependence of the diffusion coefficient for water in NafionTM.

While the interactions of water with NafionTM have been the subject of extensive study, the interactions of liquids, other than water, have received much less attention. Despite its highly fluorinated composition, NafionTM can undergo high levels of swelling in many organic solvents [11]. NafionTM has been dissolved in alcohol and alcohol/water mixtures for the purpose of coating electrodes [12] and for characterization by solution NMR [13]. A systematic study by Yeo on the swelling of NafionTM with various hydrogen bonding solvents provided evidence of two swelling maxima at widely separated solubility parameters [14]. This was interpreted as indicating the selective solvation of regions of differing polarity. There have also been studies of the interactions of alcohols and some other organic liquids with NafionTM as part of work on the pervaporative separation of water–alcohol mixtures [15] and the removal of trace water from nonswelling organic liquids [16].

The goal of the present work with NafionTM is to achieve an understanding of the factors controlling permeability and permselectivity. To this end, it was considered necessary to pursue a fundamental characterization of the transport behavior. Both sorption and permeation measurements were conducted over a range of vapor activities to determine sorption isotherms and concentration dependent diffusion coefficients. The experimental approach involved the development of flow methods for determining the transport parameters, in preference to the more traditional vacuum system approaches. Flow methods offer the advantage of working at atmospheric pressure with rather simple and versatile equip-

ment for the permeation measurements, especially in the design of the cell and the vapor source. Additional advantages are the ability to accommodate the dimensional changes of the membrane in response to the change in vapor concentration and to carry out permeation measurements with liquid as well as vapor.

NafionTM exhibits high permeabilities and appreciable membrane swelling with water and the alcohols. Under these conditions, there are various time dependent processes that complicate the analysis of the kinetics to obtain fundamental transport parameters. Therefore, the work reported here emphasizes the determination of diffusion coefficients from steady state permeabilities combined with solubilities from equilibrium vapor sorption measurements. However, due to the high permeation rates, corrections are required for the gas phase boundary layer resistance to arrive at accurate values of the diffusion coefficient [17]. Two methods are considered for correcting the boundary layer resistance: the first involves a simple correction for the boundary layer resistance to obtain nominal diffusion coefficients (D_{nom}); and the second involves more extensive corrections to obtain an effective diffusion coefficient (D_{eff}). Since the analysis and experimental procedures are treated in detail elsewhere [18], these topics are addressed only briefly in this paper. The emphasis is on the experimental results obtained for the NafionTM films with water and several alcohols.

2. Experimental details

2.1. Materials

NafionTM films (DuPont) in three thicknesses, 51 μm (NafionTM 112), 127 μm (NafionTM 115) and 178 μm (NafionTM 117) were obtained from CG Processing, Inc. Although there is some evidence that the history of the sample can affect the structure and the properties of NafionTM, a standardized method for the pretreatment of samples prior to study has yet to be adopted [3]. In most cases the samples for the present work were used without additional treatment. The neglect of an acid treatment to ensure complete conversion to the acid form might leave a small amount of alkali metal counterions, which are reported to reduce the solubility of water and alcohols in NafionTM [19]. In work to be reported in a later publication it was found that as much as 8% of low molecular weight polymer could be leached out in strongly swelling alcohol/water mixtures, to yield a film which exhibits a lower permeation rate for water. Due to difficulty in obtaining highly reproducible data with water, some of the 178 μm permeation samples were treated with aqua regia, as noted in Section 3.6. The diffusion coefficients were similar to values obtained with the untreated samples, but were more self-consistent in repeated runs.

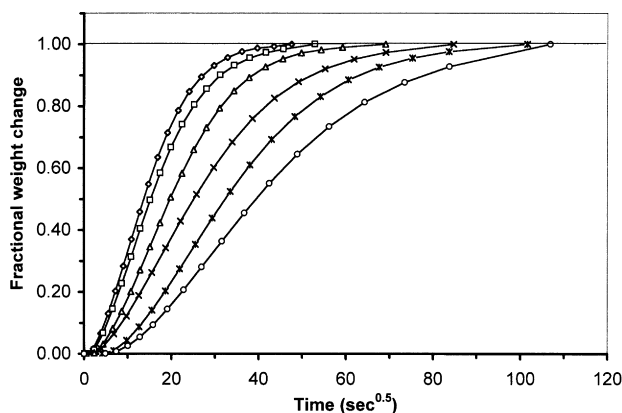


Fig. 1. Incremental sorption kinetics showing progressive decrease in rate with increasing vapor concentration. Water vapor activities for curves from left to right; 0.40, 0.60, 0.70, 0.80, 0.90, 0.95, 0.98.

Reagent grade alcohols (methanol, ethanol, 1-propanol), were used without further purification. However, after discovering that trace amounts of water greatly increased the solubility of the alcohols in Nafion™, measurements were carried out with carefully dried solvents and with molecular sieve 3A layered in the bottom of the screw capped vials used to determine immersion solubilities. Solubilities were determined at several temperatures by incubating the vials in a temperature-controlled bath. The samples were blot dried and transferred to a tared weighing bottle for weighing. Although a stable value was obtained within 1 h, the determinations were repeated over several additional time intervals. No differences were found at 20 and 32°C, the two temperatures important to the present study. The solubilities in Nafion™ 117 are as follows: water, 22.0 g/g; methanol, 49.2 g/g; ethanol 45.0 g/g; propanol 48.6 g/g. Values for the alcohols are lower than those reported by Yeo: methanol, 54 g/g; ethanol 50 g/g; propanol 55 g/g, probably due to his use of liquids that were not completely free of water, as well as possible differences in the composition of the polymer which he used [11].

2.2. Flow permeation and sorption methods

The flow permeation and sorption methods are only briefly summarized here, since most aspects have been treated elsewhere [18,20,21]. Permeation measurements were carried out with carrier and sweep flow rates of 1000 ml/min (1660 cm/min) and an exposed sample area of $6.0 \times 10^{-4} \text{ m}^2$ ($0.75 \times 1.25 \text{ in.}$). Solvent vapor was generated by a bubbler or series of bubblers, located with the sample cell in an air thermostat at 32°C. The required concentrations were produced by the mixing ratio between the saturated vapor stream from the bubbler and the dilution nitrogen gas stream, as set by mass flow controllers. Permeate concentrations were monitored by a thermal conductivity-based auto sampling analyzer (Micro Sensor Technologies, Inc., now Hewlett–Packard Co.). Samples

were usually presoaked briefly in methanol or water and dried while clamped in the cell, with the goal of reducing expansion and membrane deformation at higher vapor concentrations or with liquid exposure. Since the drying step usually caused some thinning of the exposed sample area, the thickness of the dry membrane measured after the run was used in the subsequent calculations. Boundary layer resistances for water and the alcohols were determined from measurements at two vapor activities with single and multiple stacked layers of a microporous Teflon film. The boundary layer resistance was taken as the intercept at zero film thickness.

Sorption isotherms were determined with a Cahn 2000D microbalance, which was controlled by a computer interface and software developed by Hidden Analytical. The computer program automatically proceeds through a preset series of vapor concentrations and acquires data for the weight, temperature and gas flow rates as a function of time. Solvent vapor at the required concentrations was generated by active control of the mixing ratio between the saturated vapor stream from the bubbler and the dilution gas stream at a total flow rate of 500 ml/min. The bubbler was thermostatted by immersion in a circulating refrigeration bath at 20 or 32°C. The sample was suspended inside a thermostatted, water jacketed chamber, maintained at 20 or 32°C and the entire assembly was housed in a cabinet for protection from drafts. The samples were usually dried in a 95°C oven for a preliminary weighing, and then suspended on the balance and dried overnight in a flowing stream of dry nitrogen gas before starting the run.

3. Experimental results

3.1. Sorption kinetics

For low resistance membranes there are two effects which complicate the determination of diffusion coefficients from the rate of approach to equilibrium. First, there are limitations imposed by the rate of vapor transfer across the boundary layer [22] and second, with water as well as the alcohols, there are nonisothermal conditions, due to the temperature transients accompanying sorption and desorption of vapor [23–25]. Nonetheless, it was expected that the kinetics would provide at least a qualitative indication of the trend in the diffusion coefficient with changing concentration. An example of the sorption kinetics for the 178 μm film over the range of activities, 0.4 to 0.98, appears in Fig. 1. The sorption rate decreases dramatically with increasing concentration. In addition, the sorption kinetics are decidedly nonFickian, since the fractional weight gain against the square root of time shows “S” shaped curvature. If sorption were Fickian, the initial 60% or more of the fractional weight change would be linear with the square root of time, even if the diffusion coefficient were a function of concentration [26].

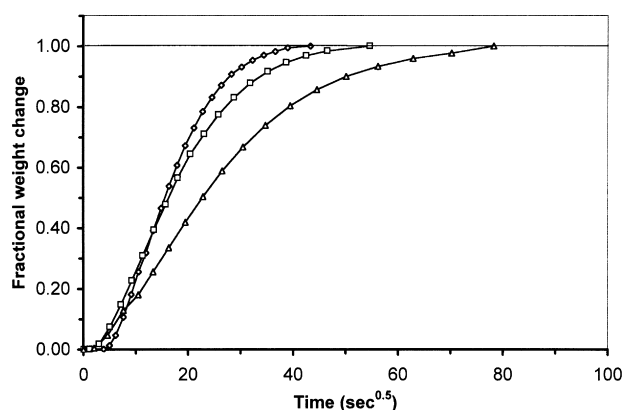


Fig. 2. Incremental sorption kinetics showing increase in rate at low vapor activities. Water vapor activities for curves from right to left; 0.05, 0.10, 0.40.

A further complication of the present data is that the desorption rates are generally higher than sorption rates, in comparisons over a fixed concentration interval. This was also noted by Morris and Sun, and by others for water vapor sorption in Nafion™. For Fickian diffusion, this implies that the diffusion coefficient decreases with concentration [26]. However, even at low concentrations where the apparent diffusion coefficient increases with concentration (Fig. 2), desorption is also faster than sorption. Approximate diffusion coefficients can be calculated from the half-time relation [26,27]:

$$D = \frac{0.0492L^2}{t_{1/2}} \quad (1)$$

where $t_{1/2}$ is the time in seconds to reach one-half of the equilibrium weight gain and L is the thickness in centimeters. For the initial step, from an activity of 0–0.05 (0.8% g/g), the apparent diffusion coefficient on sorption is 7.7×10^{-9} and 2.6×10^{-8} cm²/s on desorption. The cross-over point, where the sorption rate begins to decrease with increasing concentration, occurs above an activity of about 0.40, but desorption rates faster than sorption are observed over the entire range of measurements.

Further evidence of nonFickian behavior was provided by a comparison of the sorption kinetics for water vapor carried out on a 178 μ m and on a 356 μ m, two layer film. The rate of sorption against the reduced time coordinate, $t^{1/2}/L$, should be independent of thickness. However, the sorption rate on the reduced time scale was much faster for the 356 μ m than the 178 μ m film at the various vapor concentrations. As an example, at an activity of 0.5, the apparent diffusion coefficient from the half-time relation, was 8.98×10^{-8} for the 178 μ m film and 1.67×10^{-7} for the 356 μ m film.

Under vacuum conditions, where boundary layer transfer is not a problem, nonFickian behavior is generally a result of diffusion coupled with a relaxation process. The possible

relaxation processes include a temperature transient and a physical relaxation. Temperature transients occurring during the sorption and desorption of water, are well established in the literature [23,25] and there is increasing evidence for similar phenomena with organic vapors as well [28,29]. The effects include “S” shaped kinetics, sorption or desorption rates that decrease with increasing concentration and rates which increase with thickness on a thickness reduced time scale. However, the limitations of vapor transfer across the boundary layer can also produce anomalies, as shown by a solution to the diffusion equation under these conditions [22]. Since, the kinetics is coupled with both nonisothermal and boundary layer effects reliable diffusion coefficients cannot be obtained from the kinetic data.

An explanation for desorption rates faster than sorption rates requires that the nature of the nonisothermal effects on diffusion be considered in more detail. On sorption, there is an increase in temperature, due to the heat of condensation of the vapor, which has the effect of lowering the vapor activity relative to the higher membrane temperature, therefore, decreasing the sorption rate. On desorption, the decrease in membrane temperature will equal the increase on sorption. The lower membrane temperature, compared to the vapor, will have the effect of increasing the vapor activity, thereby slowing the desorption rate. There will be little direct effect of these temperature variations on the diffusion coefficient, due to the low activation energy of diffusion [9]. Since, the rates of sorption and desorption will be coupled with the relaxation of the temperature excursion and will be very nearly equal, another explanation must be found for desorption rates that are faster than sorption rates. The behavior is best explained by a slow volume relaxation in response to the change in vapor concentration. Relaxation processes can lead to nonFickian sorption curves under more severe conditions [30,31] and may contribute to the nonFickian behavior with the alcohols, which reach higher swelling ratios than water. The elevated desorption rates are due to the excess free volume from the preceding

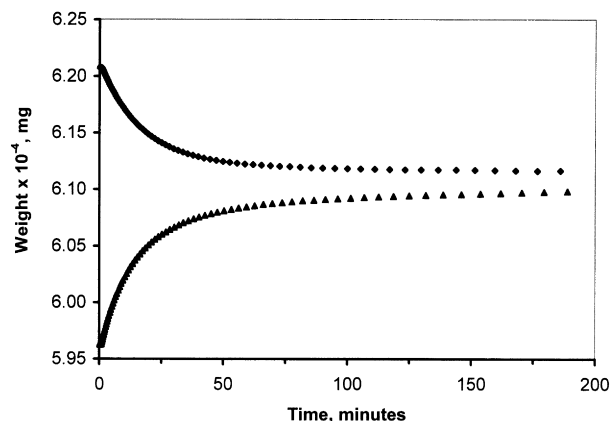


Fig. 3. Water vapor sorption, desorption kinetics, activity 0.8 to 0.9, illustrating the slow approach to equilibrium.

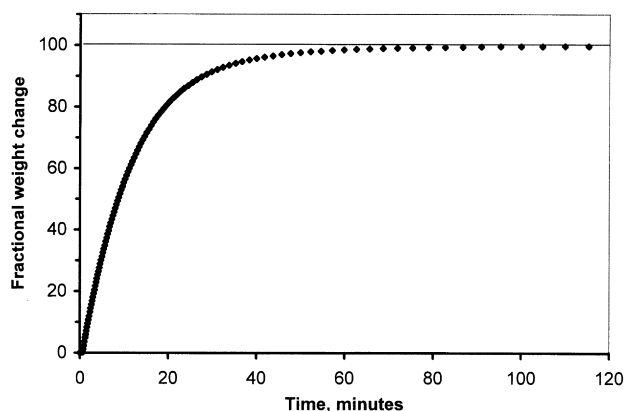


Fig. 4. Desorption kinetics, ethanol vapor, activity 0.7 showing absence of extended approach to equilibrium.

higher solvent concentration. In precise sorption and desorption runs, this relaxation process can be observed directly as a slow final approach to equilibrium (Fig. 3). However, given sufficient time there does not appear to be irrecoverable effects from the exposure to water vapor. The generally observed decrease in the sorption rate with increasing concentration is due to nonisothermal conditions and to the increasing upward curvature of the sorption isotherm at activities approaching saturation.

With the alcohols, some of the features observed in the sorption kinetics with water are also present, but there are important differences. The rate of sorption with ethanol is much lower than with water and the kinetics do not show the pronounced “S” shaped curvature seen with water (Fig. 4). The diffusion coefficient goes through a maximum at

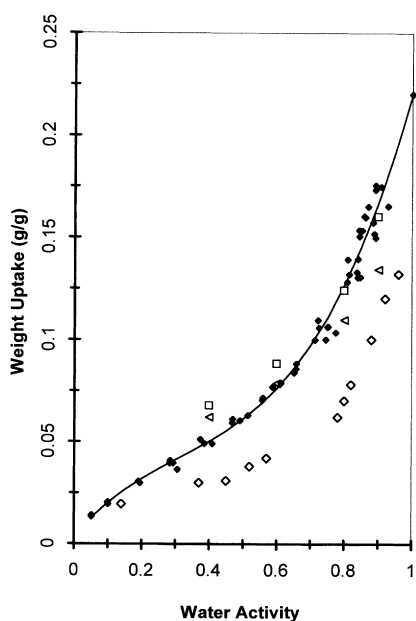


Fig. 5. Comparison of sorption isotherms for water. Starting with the highest points; open boxes [32]; open triangles [8]; filled diamonds, this work; open diamonds [10].

0.12–0.14 g/g. At the lower concentrations, the diffusion coefficient on desorption is higher than on sorption, but with increasing concentration the difference gradually diminishes and the two values merge at about 0.18 g/g. As with water, these effects can be attributed to temperature transients and relaxation behavior. Although the heat of vaporization is substantially less than that of water, the sorption isotherm is much steeper. This can result in a larger weight change for a given temperature change at the higher vapor activities and is responsible for the decreasing diffusion coefficient for ethanol with increasing concentration. The behavior with methanol and propanol is qualitatively similar to that of ethanol.

3.2. Sorption isotherms

The sorption isotherm for water at 20°C is shown in Fig. 5 along with other data from the literature [8,10,32]. The filled points represent the present experimental data, the final point is the immersion solubility and the continuous line represents the least squares third-order polynomial fit to this data. The sorption isotherm is characteristic of a swelling solvent, with an extended region of gradually increasing slope that turns more steeply concave upward above an activity of about 0.7. At the origin, the isotherm starts with a higher initial slope that levels off at an activity of 0.2, corresponding to a weight uptake of 0.03 g/g. As shown in Fig. 5, the present isotherm is in general agreement with published results from two laboratories, but much higher than the results of Zawodzinski et al. [10]. There is some indication that the solubilities at low activities in the published data are somewhat higher than the present values, suggesting an even higher initial slope. The high initial slope is in keeping with the higher hydration energy of the first 8% of water required to fill the sulfonic acid hydration shell [33]. Limited measurements were also made at 32°C in the present study. Like the immersion measurements, the sorption isotherm determined at 32°C essentially duplicated that determined at 20°C.

The sorption isotherms for the alcohols, are collected in Fig. 6 together with a comparison of the isotherm for water. The continuous line represents the third order polynomial fit, which provides a good representation of the data over most of the activity range but falls five percent below the immersion value for propanol. The isotherms show some distinctive and unexpected features. Despite the near identical saturation concentrations, the solubilities differ over most of the range of vapor activities, decreasing in the order propanol, ethanol and methanol. This is the reverse of the order that would be expected if the solubilities were strongly influenced by the hydrogen bonding capacity of the alcohols. Since the solubilities are lowest for methanol, the curve representing the sorption isotherm must cross the isotherms for the other two alcohols to meet the saturation concentration, which is nearly the same as that of propanol. In other respects these isotherms resemble that

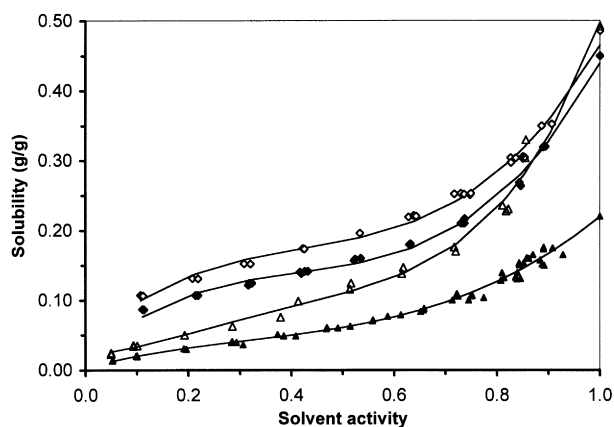


Fig. 6. Sorption isotherms, water and alcohols. Starting with the highest curve; open diamonds, propanol; filled diamonds, ethanol, open triangles, methanol; filled triangles, water.

of water. There is an extended region of gradually increasing slope, but with a more marked upturn at high activities, consistent with the more than two-fold higher solubility. There are qualitative differences between the isotherms for water and for propanol and ethanol at the lower activities, where the alcohol concentration is already about twenty percent of the saturation value at an activity of 0.1. Even though data is absent below this activity, the weight uptake must increase rapidly from the origin to meet the first experimental point. The weight uptake of 0.102 and 0.087 g/g for propanol and ethanol at activity 0.1, corresponds to about two molecules per sulfonic acid residue, far lower than the hydration shell of five for water. The initial slope of the isotherm for methanol is lower than that of the two other alcohols and somewhat closer to that of water.

3.3. Permeation kinetics

Where time dependent effects are absent, the diffusion coefficient can be determined directly from the permeation rate without requiring a knowledge of the solubility

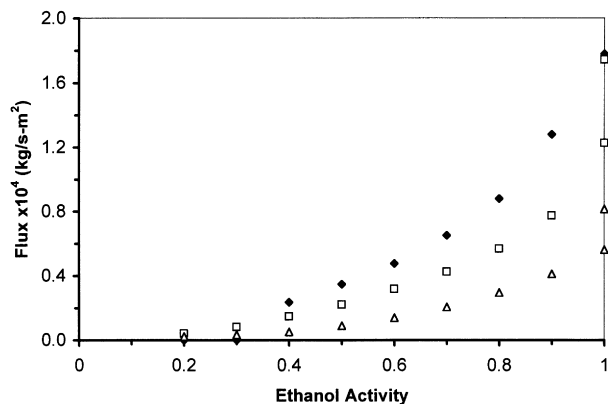


Fig. 7. Flux versus activity for three sample thicknesses, ethanol vapor and liquid. Original 127, 178 and 356 μm . Adjusted thicknesses 106.7, 175.3 and 284.5 μm .

[27,34,35]. Special precautions are required with water, even with vacuum permeation measurements [25]. Additionally, the solubility, in the form of the concentration gradient, can be determined from the ratio of the steady state permeability to the diffusion coefficient. The kinetically determined concentration gradient in a heterogeneous system incorporates the dependence on the accessible volume fraction and tortuosity. Comparison with the equilibrium solubility from the sorption isotherm should provide a measure of the concentration-scaling factor due to the impermeable fluorocarbon fraction. However, the limitations affecting the determination of diffusion coefficients from the sorption kinetics also apply to the permeation kinetics, particularly the problems of boundary layer transfer and the temperature transients arising on sorption or desorption of the vapor. Examples of directly measured temperature changes which accompany step changes in water vapor activity are provided elsewhere [18].

To reduce the boundary layer and nonisothermal problems with water, in one experiment the time scale for diffusion was increased by using four layers of the 178 μm NafionTM film. Nonetheless, there was evidence of nonFickian behavior, in the slow approach to steady state when compared to the theoretical permeation kinetics for the coefficient diffusion. As an example, at a water vapor activity of 0.7 the best fit of the theory [34] to the experimental kinetics gave a diffusion coefficient of $4.3 \times 10^{-7} \text{ cm}^2/\text{s}$ and a corresponding solubility of 0.16 g/g. The diffusion coefficient is about half that determined from steady state measurements, discussed below, and the kinetically determined solubility is about 60% higher than the value from sorption equilibrium. However, it is not possible to accept this difference in solubilities as a measure of the increased concentration in the accessible fraction of NafionTM, due to the expected nonisothermal and the relaxation effects on the diffusion coefficient from the permeation kinetics.

3.4. Steady state permeation; nominal diffusion coefficients

The flux of ethanol in the films of three different thicknesses as a function of vapor activity is shown in Fig. 7. The use of vapor activity rather than the usual units of membrane concentration provides a perspective about the data in its original form, since the permeation runs are set up in terms of a series of vapor activities. The flux increases continuously as a function of activity with a gradual concave upward curvature. The curves for the three different films are similar, well separated, and in the expected order. Note that there are two values at unit activity, the lower for the vapor and the higher point for the liquid. The flux for liquid in the 127 μm film is off scale at a value of $2.8 \times 10^{-4} \text{ kg/s m}^2$. One of the challenges of the data analysis is to develop a reasonable correlation for the flux at unit activity vapor and the much higher flux that occurs with the liquid. The results for the other alcohols and water are similar, except for the differences in the magnitude and

Table 1
Comparison of results from steady state permeation

	P/P_0	Flux (kg/s m^2)	Resistance (s/m)	Ratio (R_{bl}/R_t) (%) ^a
Water, 356 μm	0.4	9.65×10^{-6}	834	11.6
$R_{bl} = 97 \text{ s/m}$	1.0	2.82×10^{-6}	244	39.8
	Liquid	1.18×10^{-6}	102	95.1
Methanol, 127 μm	0.5	1.80×10^{-5}	1560	8.7
$R_{bl} = 135 \text{ s/m}$	1.0	7.81×10^{-6}	675	20.0
	Liquid	4.17×10^{-6}	360	37.5
Ethanol, 178 μm	0.2	1.19×10^{-4}	10265	1.4
$R_{bl} = 146 \text{ s/m}$	1.0	1.90×10^{-5}	1645	8.9
	Liquid	1.32×10^{-5}	1164	12.5
Propanol, 127 μm	0.2	7.69×10^{-5}	6646	3.5
$R_{bl} = 233 \text{ s/m}$	1.0	1.79×10^{-5}	1550	15.1
	Liquid	1.05×10^{-5}	923	25.3

^a Ratio of boundary layer resistance to total resistance.

slope of the flux versus activity, which is highest for water and lowest for propanol.

The measured permeability can be characterized by a resistance which is determined by the ratio of the gas phase concentration driving force to the flux (Eq. (2)):

$$R = \frac{\Delta C}{J} \quad (2)$$

When the flux, J , is in units of $\text{kg/m}^2/\text{s}$ and ΔC in units of kg/m^3 , R has units of s/m. The measured resistance is the sum of the boundary layer resistance and the membrane resistance. If the membrane resistance is very high compared to the boundary layer resistance, the correction for the boundary layer resistance can be neglected and, in practice, is often neglected even when this condition is not strictly met. However, for conditions of high membrane permeability, an improved approximation to a concentration dependent diffusion coefficient can be obtained by subtracting the boundary layer resistance from the measured resistance to obtain a value for the membrane resistance. The membrane resistance is converted to an adjusted flux

using Eq. (2), and the diffusion coefficient D (cm^2/s) is calculated from Fick's law relation, Eq. (3). Here ΔC is the concentration gradient in the membrane, determined from the sorption isotherm and L is the membrane thickness.

$$J = D \frac{\Delta C}{L} \quad (3)$$

Since the concentration defined by the sorption isotherm is a nominal concentration, corresponding to the set vapor activity, the diffusion coefficient from this procedure is referred to as a nominal diffusion coefficient, D_{nom} . Table 1 presents a selection of characteristic permeation data for water and the three alcohols, including the ratio of boundary layer to total resistance for different conditions. The comparisons indicate that the boundary layer resistance is an appreciable fraction of the measured resistance, particularly for the thinner films and for the higher vapor activities.

Values of D_{nom} for ethanol in Fig. 8, exhibit an unusual trend with concentration, common to all three sample thicknesses. D_{nom} increases rapidly at a concentration of about 0.2 g/cm^3 , but levels off above 0.4 g/cm^3 to a nearly concentration independent plateau. There is also an indication of a transition to a region of very low slope for D_{nom} at the lowest concentrations. This structure in the concentration dependence of the diffusion coefficient contrasts with the smooth increase in diffusion coefficient for swelling solvents in nonphase segregated elastomers. The values of D_{nom} for liquid ethanol are higher than for the unit activity vapor, an indication of the limitation of this simple analysis. The curves for the three different thicknesses samples are in reasonable agreement, supporting the assumption of Fickian behavior. The small differences with film thickness could be due to any of several factors, but evidence to be presented later indicates that the sample properties may not be identical. Although not shown, the concentration dependence of D_{nom} for methanol and propanol is similar to the pattern for ethanol. The concentration dependence of D_{nom} for water also exhibits some similarities to ethanol (see Fig. 11). The diffusion coefficient increases rapidly at

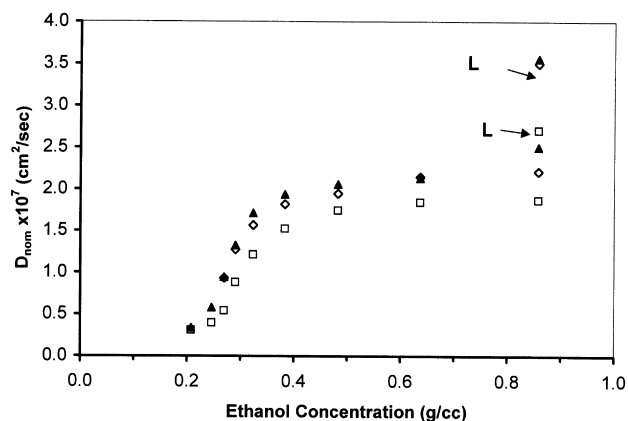


Fig. 8. D_{nom} versus concentration, ethanol vapor and liquid for three sample thicknesses: original 127, 178 and 356 μm ; adjusted thicknesses 106.7, 175.3 and 284.5 μm .

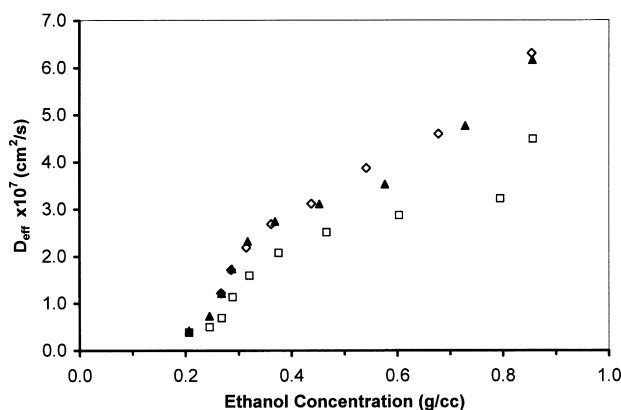


Fig. 9. D_{eff} versus concentration, ethanol vapor and liquid for three sample thicknesses: original 127, 178 and 356 μm ; adjusted thicknesses 106.7, 175.3 and 284.5 μm .

concentrations above 0.06 g/cm^3 and appears to nearly level out above a concentration of about 0.25 g/cm^3 . There are two widely separated values of D_{nom} at the final concentration of 0.43 g/cm^3 , which correspond to the unit activity vapor and the liquid. It is to be noted that the plateau values of D_{nom} for water are about seven-fold higher than the plateau values for ethanol. It will be shown in the later, more detailed analysis that the similarities between the concentration dependence of D_{nom} for water and ethanol are a consequence of the limitations of the present analysis at the much higher permeation rates of water. Despite these limitations, the distinctive “S” shaped concentration dependence of D_{nom} , for ethanol will prove to be characteristic for the three alcohols, although not for water.

3.5. Steady state permeation: analysis for effective diffusion coefficients

In proceeding to a more accurate treatment of the permeation data it is necessary to apply two types of correction. The procedure is presented in detail elsewhere [18] so that only a brief description of the process is given here. First, there is a

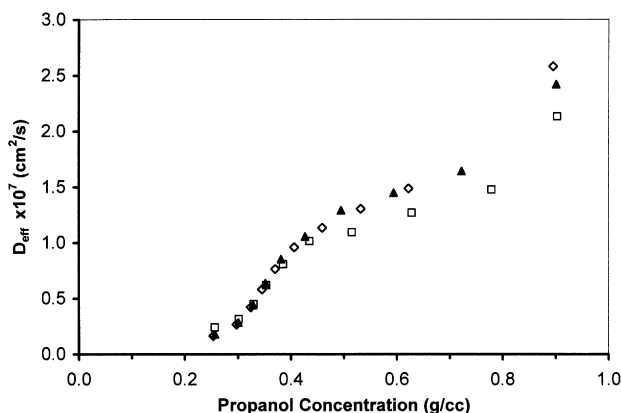


Fig. 10. D_{eff} versus concentration, propanol vapor and liquid for three sample thicknesses: original 51, 127 and 178 μm ; adjusted thicknesses, 1.85, 4.20 and 6.25 μm .

correction for the depletion of the vapor concentration from the carrier stream and for the accumulation of vapor in the sweep stream with flow along the length of the sample. Second, there is an important correction for the change in gas phase concentration across the boundary layer resistance which determines the vapor concentration at the membrane surface [36]. The surface vapor concentration is converted to a concentration difference across the membrane ΔC , at the inlet and outlet ends of the membrane using a polynomial fit to the sorption isotherm. The inlet and outlet concentration differences are subjected to a log normal average:

$$\overline{\Delta C} = (\Delta C_{\text{in}} - \Delta C_{\text{out}}) / \ln (\Delta C_{\text{in}} / \Delta C_{\text{out}}) \quad (4)$$

$\overline{\Delta C}$ is treated as the effective concentration corresponding to the set vapor activity.

The diffusion coefficient is calculated as the ratio of the measured flux to the effective concentration gradient $\overline{\Delta C}/L$. The resulting value is adjusted for the change in thickness due to solvent swelling, assuming that all swelling occurs in the thickness direction, since the membrane is clamped on its periphery. The swelling concentration is taken as one half the sum of $\overline{\Delta C}$ and the concentration at the lower membrane surface, which is equivalent to the assumption of a linear concentration gradient in the membrane. The resulting value is an effective diffusion coefficient, D_{eff} , which corresponds to an average over the concentration difference between the upper and lower membrane surfaces:

$$\bar{D} = \frac{1}{C_1 - C_2} \int_{C_2}^{C_1} D(C) dC \quad (5)$$

If C_1 is zero, then D_{eff} can be treated as a function solely of the upper surface membrane concentration. Since the downstream membrane concentration is not zero, D_{eff} is plotted at an adjusted concentration, which is the sum of $\overline{\Delta C}$ and one half the concentration at the lower membrane surface. In addition, a correction could be applied to adjust the D_{eff} values at different concentrations to the same downstream concentration, ideally zero. Although the data has not been adjusted in this fashion, it will be seen that the resulting values of D_{eff} provide a consistent representation of the diffusion coefficient, in terms of both the concentration dependence and relative magnitude for the different liquids.

3.6. Steady state permeation: comparison of effective diffusion coefficients

Values of D_{eff} as a function of concentration appear in Fig. 9 for ethanol in the three different thickness NafionTM films. The results indicate the effect of the corrections for the concentration changes across the boundary layer resistance. The corrections are greatest for the 127 μm film, due to the higher flux which results in larger concentration changes across the boundary layer resistance. The main feature which appears in D_{nom} , the rapid increase in the concentration interval, $0.2\text{--}0.4 \text{ g/cm}^3$, is also prominent in

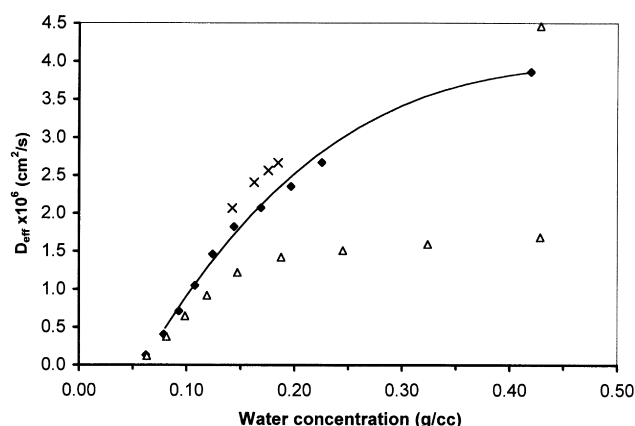


Fig. 11. Diffusion coefficients versus concentration for water: open triangles, D_{nom} , two layer 178 μm film; filled diamonds, D_{eff} , two layer 178 μm film; crosses, D_{eff} , multilayer 178 μm films, vapor activity 0.8.

the D_{eff} values. However, there is now a pronounced positive slope rather than a plateau at higher concentrations. This is due to the fact that the values of D_{eff} are higher than D_{nom} and shifted to lower concentrations for equal vapor activities. The values of D_{eff} for the liquid are still higher than values for the vapor at unit activity but the results for the two thinner films appear to follow a consistent trend of a smoothly increasing slope. There is still an unresolved problem with the results for the thickest film, which lie well below the other values and for which there is a larger difference between the unit activity vapor and liquid. Since the values of D_{nom} for this sample are also lower than for the other two films, the difficulty probably resides in the original data rather than the analysis. The results for propanol, plotted in Fig. 10, show the same main features as the ethanol data. In this case there is closer agreement in D_{eff} for the films of three thicknesses, however, there is a somewhat greater difference between the values of D_{eff} for the vapor and liquid than with ethanol. There is reason to believe that this increase in the slope of D_{eff} is reliable since this does not occur with water, which is the

most severe test of the boundary layer corrections (see Table 1).

A useful comparison can be made of the values of D_{eff} for ethanol with apparent diffusion coefficients from sorption kinetics at the lowest concentrations, where nonisothermal effects are minimal. At a concentration of 10.6%, D_{eff} is $4.2 \times 10^{-8} \text{ cm}^2/\text{s}$, which is equal to the average of the values from the sorption and desorption kinetics at this concentration. At the next higher concentration, which is at the maximum in the sorption kinetics, D_{eff} is about 30% higher than the desorption value from the kinetics. The correspondence between the two methods, although limited, provides support for the magnitude of D_{eff} values at the low concentrations. In the measurements with water, there was difficulty in reproducing the data for the liquid, which is a critical value, due to the effect of the low membrane resistance in limiting the accessible range of concentrations. The usual method of sample conditioning, in which the sample was briefly presoaked in methanol or water and dried while clamped in the cell, resulted in the sample buckling at the highest vapor activities, as well as with liquid water. To avoid this problem, the sample was installed wet and the upper surface was supplied with water while the bottom surface was swept with dry nitrogen in the approach to steady state. When removed from the cell, the sample was flat and after drying the thickness was close to the original value. This method provided good reproducibility in four repeat measurements on 178 μm films with liquid water, each with a new sample.

The results of the run with two layers of 178 μm , aqua regia treated film appear in Fig. 11. The D_{eff} values are a strongly increasing function of concentration and appear to merge smoothly with the value for liquid water. However, it is not possible to completely rule out that D_{eff} could follow a lower slope between the unit activity vapor and the liquid. If this possibility is ignored, the data can be conveniently fitted by a third-order polynomial, represented by the continuous curve in Fig. 11. Although, the curve approaches an intercept on the concentration axis at five percent, which would

Table 2
Calculation of effective diffusion coefficients

P/P_0	Flux (g cm/s cm^2)	Long mean conc. (g/ml)	D (cm^2/s)	Eff. conc. (g/ml) ^a	Deff adj. thick (cm^2/s) ^b
0.2	7.39×10^{-9}	0.059	1.26×10^{-7}	0.062	1.29×10^{-7}
0.3	2.80×10^{-8}	0.073	3.86×10^{-7}	0.079	4.02×10^{-7}
0.4	5.60×10^{-8}	0.083	6.74×10^{-7}	0.093	7.05×10^{-7}
0.5	9.23×10^{-8}	0.094	9.86×10^{-7}	0.108	1.04×10^{-6}
0.6	1.43×10^{-7}	0.105	1.36×10^{-6}	0.124	1.45×10^{-6}
0.7	2.00×10^{-7}	0.119	1.68×10^{-6}	0.144	1.80×10^{-6}
0.8	2.63×10^{-7}	0.139	1.88×10^{-6}	0.169	2.04×10^{-6}
0.9	3.41×10^{-7}	0.162	2.11×10^{-6}	0.197	2.31×10^{-6}
1.0	4.35×10^{-7}	0.185	2.35×10^{-6}	0.226	2.62×10^{-6}
Liquid	1.00×10^{-6}	0.327	3.07×10^{-6}	0.420	3.72×10^{-6}

^a The effective concentration is taken as the log mean concentration plus one-half the lower surface membrane concentration.

^b The thickness correction assumes that the average membrane concentration is one-half the sum of the log mean concentration and the lower surface membrane concentration and that all swelling occurs in the thickness direction in the clamped sample.

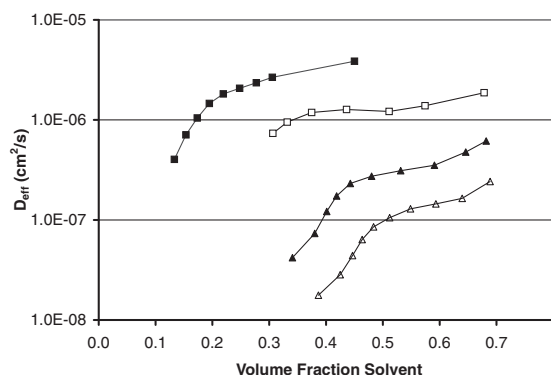


Fig. 12. Comparison of D_{eff} versus solvent volume fraction; water and alcohols: filled square, water; open square, methanol; filled triangle, ethanol; open triangle, propanol.

correspond to about two water molecules per sulfonic acid, the limited data at the lowest concentrations appears to continue at a much lower slope, similar to the behavior for ethanol. With the high heat of vaporization for water, there is the possibility of a temperature gradient across the membrane at steady state. The calculation is easily carried out for the steady state conditions and was found to be insignificant for the film thickness used in this run. A direct comparison of D_{eff} with D_{nom} values, open points, indicates the striking difference that is produced by the more detailed boundary layer corrections. In view of the importance of the diffusion data for water in NafionTM, the related values are provided in Table 2.

3.7. Steady state permeation: tests of thickness dependence

A series of measurements was made on multilayer 178 μm films, used as received, with water vapor at activity of 0.5 and 0.8, to test the applicability of the thickness scaling of the permeation rate, and also test for inherent differences in the samples of different thickness. The results of a set of measurements at activity 0.8 on multilayer 178 μm film samples, from one to four layers, is represented by the crosses in Fig. 11. The multilayer values increase progressively with increasing thickness, due to the progressively smaller change in vapor concentration across the boundary layer with increasing membrane resistance. The set of four points fall parallel to the values for D_{eff} with the two-layer sample, but offset to higher values by about 20%. The results for the other film thicknesses also follow a similar trend of increasing D_{eff} values with increasing thickness, validating the assumption of linear scaling of the steady state permeation rate with thickness, as required by Fick's law behavior. Although the results for the 178 μm films were only slightly lower than the values for the 127 μm films, the D_{eff} values for the 51 μm films at activity 0.5 and 0.8 were much lower. This suggests that there is a difference in the film properties, probably associated with the diffusion coefficient for the 51 μm film, since the immersion solubility was the same in all three films. In

contrast to these results with water, the data for propanol in Fig. 10 show good agreement for the 51 and 127 μm films while the data for the 178 μm film is somewhat lower.

3.8. Steady state permeation: additional diffusion coefficient comparisons

A comparison of the results for water and the alcohols appears in Fig. 12, in a log plot as a function of the solvent volume fraction. Data for methanol, although limited to the 127 μm film, and associated with large values of the flux and the related corrections, are also included. This comparison emphasizes certain similarities, and suggests that there is a progressive change in the nature of the concentration dependence for water and the series of alcohols, from methanol to propanol. A comparison of values of D_{eff} for the different solvents can be made in the limited concentration range at a volume fraction of 0.45, where data for water and methanol and ethanol overlap, and at a value for propanol just below the change in slope. The values, are approximately in the ratio of 5.8, 17.1, 3.8, 1.0 for water, methanol, ethanol, propanol. From simple geometric considerations the diffusion coefficients might be expected to scale with the reciprocal of the molecular volumes. Using molecular volumes based on van der Waals radii, which are close to the values from density, the product of the diffusion coefficients and the estimated molecular volumes for water and for the alcohol is in the ratio of 11.3, 7.8, 2.2, 1.0. These results show the sensitivity of D_{eff} to molecular size, and the selectivity of NafionTM for water and, to a lesser extent, for methanol. The differences are magnified in the low concentration region by the rapid drop off in D_{eff} for the alcohols compared with the trend for water.

As a test of the validity of the analytical procedure, comparisons can be made of the diffusion coefficient for water from the steady state permeation measurements and immersion values. An immersion value of $2.3 \times 10^{-6} \text{ cm}^2/\text{s}$ at 32°C was determined on a 1270 μm film in Eisenberg's laboratory [9]. This value compares with a diffusion coefficient of $1.7 \times 10^{-6} \text{ cm}^2/\text{s}$ at 30°C, determined in this work by sequential vapor permeation measurements on a set of 178 μm samples. The value of D_{eff} determined with liquid water is $3.86 \times 10^{-6} \text{ cm}^2/\text{s}$. D_{eff} is an average over a concentration range similar to that in the immersion measurement. However, the immersion value must be corrected for the time dependent dimensional change accompanying the water uptake. Assuming that swelling is limited to the thickness direction, and applying the correction factor $1/\phi_2^2$, where ϕ_2 is the volume fraction of polymer [26,27], the immersion value falls between 3.3×10^{-6} and $4.4 \times 10^{-6} \text{ cm}^2/\text{s}$. The close match of the steady state and the immersion values is somewhat fortuitous, since the several underlying approximations are open to question, but at least the comparison indicates that the two values are of similar magnitude.

Another interesting comparison can be made between D_{eff}

and the percolation threshold for conductivity. Nafion™ is a proton conductor with a transference number of 2.6 water molecules per proton and the conductivity exhibits a strong dependence on water content. The threshold water concentration occurs at a volume fraction of about 0.1, which corresponds to 0.12 g/cm^3 [37]. There is no similar critical effect at this concentration in D_{eff} , which is already fairly high, $1.3 \times 10^{-6} \text{ cm}^2/\text{s}$ at this concentration. D_{eff} decreases smoothly over a range of experimentally determined values at lower concentrations (see Fig. 11), which extend just past the apparent intercept of the fitted polynomial at a concentration of about 0.05 g/cm^3 .

4. Discussion

The primary goal of the present study is to gain an improved understanding of the transport behavior of water and alcohols in Nafion™ by determining sorption isotherms and concentration dependent diffusion coefficients. Previous studies on the diffusion of water in Nafion™ [8,10] found that the diffusion coefficient goes through a maximum at low concentrations, is higher on desorption than on sorption and that the average value is well below the reported immersion value [9]. In the present work it is shown that these results can be explained by time dependent processes which are coupled with the diffusion kinetics, and by vapor phase mass transfer limitations. The relaxation of temperature transients accompanying the sorption or desorption of water results in apparent diffusion coefficients that are lower than the correct values. Since the magnitude of the nonisothermal effect increases with concentration, due to the increasing slope of the sorption isotherm, which largely determines the temperature coefficient of the concentration change, the diffusion coefficient appears to decrease with increasing concentration. In addition, a time dependent volume relaxation is evident in the slow approach to sorption equilibrium and to steady state permeation. That the desorption kinetics are faster than the sorption kinetics is due to the excess free volume introduced at the higher water content of the prior step in the run. The difficulties introduced by the temperature excursion, the volume relaxation, and in the case of the flow methods, vapor transfer across the boundary layer are avoided by determining the diffusion coefficient from the combination of the steady state permeation rate and equilibrium solubility. The resulting effective diffusion coefficient, D_{eff} , for water in Nafion™ increases monotonically and smoothly over an extended range of concentrations, which includes the value for liquid water. The diffusion coefficients at the highest vapor concentrations and for liquid water are consistent with the value from immersion measurements [9].

This study also indicates the considerable differences in solubility and diffusion behavior of water and the alcohols. The difference in the interaction of water and the alcohols with Nafion™ is evident in a solubility almost three-fold

greater for the alcohols than water on a volume basis and in the corresponding differences in the sorption isotherms. Despite the higher swelling ratio with the alcohols, Nafion™ is not soluble in the dry alcohols at elevated temperatures, whereas mixtures of water and the alcohols are known to solubilize Nafion™ at temperatures well above the boiling point of the mixtures [12]. Also, in work to be reported later, it is shown that addition of small amounts of water to alcohols results in a large increase in solvent uptake at ambient temperature. Some qualitative suggestions can be made about the specific interactions with Nafion™ that are responsible for the differences in the solubility behavior of water and the alcohols. Spectroscopic studies of Nafion™ have shown that the sulfonic acid residues are involved in strong mutual pair-wise or multiple hydrogen bonding interactions [38,39] which act as effective cross links in the absence of water, and that water interacts directly with the sulfonic acid residues. The disruption of the sulfonic acid hydrogen bonding by water probably contributes to the large increase in solubility of water–alcohol mixtures. Since alcohols appear to be less effective than water in competing with the inter-sulfonic acid hydrogen bonds, the appreciable solubility of the dry alcohols suggests that these liquids may be able to solvate the fluoroether rich regions of Nafion™. This solubility could be mediated by hydrogen bonding and polar interactions with the ether oxygen and, perhaps, also the fluorine on the unsymmetrically substituted carbon [40].

Another indication of the differences in the interactions of water and the alcohols with Nafion™ is provided by comparisons of the diffusion behavior. The diffusion coefficient for water resembles the well-documented behavior for an elastomer, since it is a smoothly increasing function of concentration [41]. The extrapolation to a near zero value at a finite concentration is probably due to immobilization of water by sulfonic acid interactions at very low concentrations. With the alcohols there are three distinct regions of behavior. At the lowest concentrations, only partly within the limits of experiment, the values of D_{eff} are low, in combination with a low slope. D_{eff} increases rapidly in a narrow concentration range starting at $0.17\text{--}0.2 \text{ g/cm}^3$ for ethanol and somewhat higher for propanol. This is followed by a semi-plateau region of a much lower slope that increases more rapidly in the approach to the liquid D_{eff} value. Since there are indications of strong interactions of water with the sulfonic acid residues, it is expected that the diffusion of water would follow ionic pathways that are accessible even at low water concentrations. If the alcohols interact primarily with the fluoroether rich regions of Nafion™, the diffusion behavior at low concentrations implies that the alcohols are localized in isolated, polar regions. The marked increase in diffusion coefficient in a narrow concentration interval at higher concentrations is consistent with a swelling mediated change in Nafion™ structure leading to an increased density of diffusion pathways through the fluorocarbon matrix. This view of alcohol induced structural change is supported by the interactions of alcohols with

Nafion™, summarized above, and by a report that swelling with ethanol can induce structural changes that persist even after the Nafion™ sample is dried and rehydrated [42].

5. Conclusions

An extensive literature exists concerning the solubility and diffusion coefficient of water in Nafion™, with apparent agreement that the diffusion coefficient of water passes through a maximum at low concentrations. In contrast the present analysis of steady state permeation combined with equilibrium solubility measurements shows that the diffusion coefficient increases monotonically with increasing concentration. The misleading diffusion coefficients and other anomalies in the kinetics are due to the failure to take proper account of nonisothermal conditions, physical relaxation processes and, in certain cases, vapor phase mass transfer. Although reliable values of the diffusion coefficient for water or the alcohols in Nafion™ cannot be determined directly from the sorption or permeation kinetics, they can be obtained from combined steady state permeation and equilibrium solubility measurements under continuous flow conditions, with proper attention to corrections for the boundary layer effects in the permeation measurements. These corrections assume critical importance for the conditions of low membrane resistance, which are of interest in this work. The current procedure represents the preferred approach for assessing the transport parameters for solvents under conditions of high flux and high swelling, which are frequently associated with nonideal kinetics due to non-isothermal conditions and other time dependent effects.

The transport behavior determined for water and the alcohols in Nafion™ highlights significant differences both in the solubility and in the concentration dependence of the diffusion coefficient, for these two classes of liquids. The alcohol solubilities are almost three times higher than the solubility of water (g/cm^3) with corresponding differences in the sorption isotherms, but the addition of small amounts of water to the alcohols can produce a significant increase in solubility. For water, the diffusion coefficient follows a smooth, monotonic increase with concentration, while for alcohols, the diffusion coefficient undergoes a large increase in a small concentration range. These differences in the solubility and diffusion behavior must arise from differences in the interaction of these two classes of liquids with Nafion™. There is spectroscopic evidence that water interacts specifically with the sulfonic acid residues and disrupts the inter-sulfonic acid hydrogen bonding. This could account for the increased solubility of water–alcohol mixtures. It is suggested in this paper that the high level of swelling by dry alcohols involves interactions with the fluoroether side chain, possibly the ether oxygen and the fluorine of the unsymmetrically substituted carbon, and that a swelling mediated change in structure is responsible for the sigmoidal concentration dependent diffusion of the

alcohols. The anomalous diffusion behavior of the alcohols cannot be treated simply in terms of Fujita free volume concepts, which apply to a polymer medium of fixed properties. To gain a fundamental understanding of the differences in diffusion behavior of water and the alcohols, requires information derived from complementary studies. Small angle X-ray measurements of water and ethanol swollen Nafion™ [43], as well as, NMR measurements of the solvent self-diffusion coefficients and the characteristic dimensions of solvent swollen Nafion™ [44], are in progress in other laboratories. The results of these cooperative studies should provide the foundation for a more detailed understanding of the factors controlling the permeability and permselectivity of Nafion™.

References

- [1] Robertson MAF, Yeager HL. In: Tant MT, Mauritz KA, Wilkes GL, editors. Ionomers, synthesis, structure, properties and applications, London: Blackie (Chapman and Hall), 1997 (chap. 7).
- [2] Ukihashi H, Yamabe M, Miyake H. *Prog Polym Sci* 1986;12:229–70.
- [3] Yeager HL, Gronowski AA. In: Tant MT, Mauritz KA, Wilkes GL, editors. Ionomers, synthesis, structure, properties and applications, London: Blackie (Chapman and Hall), 1997.
- [4] Gierke TD, Munn GE, Wilson FC. In: Eisenberg A, Yeager HL, editors. Perfluorinated ionomer membranes, ACS symposium series 180, Washington, DC: American Chemical Society, 1982 (chap. 10).
- [5] Gierke TD, Hsu WY. In: Eisenberg A, Yeager, editors. Perfluorinated ionomer membranes, ACS symposium series 180, Washington, DC: American Chemical Society, 1982 (chap. 13).
- [6] Yeager HL. In: Eisenberg A, Yeager HL, editors. Perfluorinated ionomer membranes, ACS symposium series 180, Washington, DC: American Chemical Society, 1982 (chap. 4).
- [7] Mauritz K. In: Tant MT, Mauritz KA, Wilkes GL, editors. Ionomers, synthesis, structure, properties and applications, London: Blackie (Chapman and Hall), 1997 (chap. 7).
- [8] Morris DR, Sun X. *J Appl Polym Sci* 1993;50:1445–52.
- [9] Yeo SC, Eisenberg A. *J Appl Polym Sci* 1977;21:875–98.
- [10] Zawodzinski Jr. TA, Neemand M, Silerud LO, Gottesfeld S. *J Phys Chem* 1991;95:6040–4.
- [11] Yeo RS. *Polymer* 1980;21:432–3.
- [12] Martin CR, Rhoades TA, Ferguson FA. *Anal Chem* 1982;54:1639–41.
- [13] Schlick S, Gebel G, Pineri M, Volino F. *Macromolecules* 1991;24:3517–21.
- [14] Yeo RS. *J Appl Polymer Sci* 1986;32:5733–41.
- [15] Nagahma SK, Noritomi H, Asai H. *J Membrane Sci* 1992;72:31–41.
- [16] Leckrone KJ, Hayes JM. *Anal Chem* 1997;69:911–8.
- [17] Skaarup K, Hansen CM. *Polym Engng Sci* 1980;20:259–63.
- [18] Rivin D, Gibson PW, Kendrick CE, Schneider NS, Meldon J. In preparation.
- [19] Takamatsu T, Hashiyama M, Eisenberg A. *J Appl Polym Sci* 1979;24:2199–220.
- [20] Gibson P, Kendrick C, Rivin D, Sicuranza L, Charmchi M. In: Stull JA, Schwoppe AD, editors. Performance of protective clothing, vol. 6. West Conshohocken, PA: ASTM, 1997 (ASTM STP 1273).
- [21] Gibson P, Kendrick C, Rivin D, Sicuranza L, Charmchi M. *J Coated Fabrics* 1995;24:322–45.
- [22] Nguyen TV, Vanderborgh N. *J Membrane Sci* 1998;143:235–48.
- [23] Armstrong Jr. AA, Wellons JD, Stannett V. *Makromol Chemie* 1966;95:78–91.
- [24] Ruthven DM, Lee LK. *AIChE J* 1981;27:654–62.
- [25] Paul D, Shult K. *J Appl Polym Sci* 1996;61:1865–76.

- [26] Crank J. The mathematics of diffusion. 2nd ed. Oxford: Clarendon Press, 1975 (chap. 9).
- [27] Crank J, Park GS. In: Crank J, Park GS, editors. Diffusion in polymers, London: Academic Press, 1968 (chap. 1).
- [28] Waksman LW, Schneider NS, Sung NH. In: Koros WJ, editor. Barrier polymers and structures, ACS symposium series 423, Washington, DC: American Chemical Society, 1990 (chap. 20).
- [29] Wang P, Meldon J, Sung NH. J Appl Polym Sci 1996;59:937–44.
- [30] Joshi S, Astarita G. Polymer 1979;20:455–8.
- [31] Hedenqvist MS, Gedde UW. Polymer 1999;40:2381–93.
- [32] Pushpa KK, Nandan D, Iyer RM. J Chem Soc Faraday Trans 1998;84:2047–56.
- [33] Escoubes M, Pineri M. In: Eisenberg A, Yeager HL, editors. Perfluorinated ionomer membranes, ACS symposium series 180, Washington, DC: American Chemical Society, 1982 (chap. 1).
- [34] Felder RM, Spence RD, Ferrell JK. J Appl Polym Sci 1975;19:3193–200.
- [35] Singh A, Freeman BD, Pinnau I. J Polym Sci Polym Phys 1998;36:289–301.
- [36] Rautenbach R, Albrecht R. Membrane processes. London: Wiley, 1989 (chap. 4).
- [37] Hsu WY, Barkley JR, Meakin P. Macromolecules 1980;13:198–200.
- [38] Falk M. In: Eisenberg A, Yeager HL, editors. Perfluorinated ionomer membranes, ACS symposium series 180, Washington, DC: American Chemical Society, 1982 (chap. 8).
- [39] Falk M. Can J Chem 1980;58:1495–501.
- [40] Wang P, Schneider NS, Sung NH. J Appl Polym Sci 1999;71:1525–35.
- [41] Schneider NS, Moseman JH, Sung NH. J Polym Sci Polym Phys 1984;32:481–99.
- [42] Miura Y, Yoshida H. Mem Fac Tech Tokyo Metropolitan Univ 1990;40:4349–60.
- [43] Trevino S, Young S, Beck Tan N. Private communication, 1999.
- [44] Meresig TA, Gong W-Y, Inglefield PT, Jones AA, Schneider NS. ACS Polymr Prep 1998;39(2):886–7.